An experimental and modeling study of the oxidation of 3-pentanol at high pressure

Maxime Carbonnier, Zeynep Serinyel, Alan Keromnes, Guillaume Dayma, Benoîte Lefort, Luis Le Moyne, Philippe Dagaut

An experimental and modelling study of the oxidation of 3-pentanol at high pressure

Maxime Carbonnier[1,3], Zeynep Serinyel[1,2], Alan Kéromnès[3], Guillaume Dayma[1,2], Benoîte Lefort[3], Luis LeMoyne[3] and Philippe Dagaut[1]

[1] CNRS, Institut de Combustion, Aérothermique, Réactivité et Environnement 1C, Avenue de la recherche scientifique, 45071 Orléans cedex 2, France

[2] Université d'Orléans, 6 Avenue du Parc Floral, 45100 Orléans, France

[3] DRIVE, EA1859, Université de Bourgogne-Franche Comté, 49 rue Mademoiselle Bourgeois, 58000 Nevers

*Corresponding author:
Zeynep Serinyel, PhD
CNRS–ICARE, Institut de Combustion, Aérothermique, Réactivité et Environnement
1C Avenue de la Recherche Scientifique
45071 Orléans Cedex 2, France
Tel : +33 (0)2 38 25 77 77
Fax : +33 (0)2 38 69 60 04
zeynep.serinyel@cnrs-orleans.fr

Colloquium : Gas-phase reaction

Total length of paper (method 1): 6179 Words

Main text: 2751 Words
References: (26+2) x (2.3 lines/reference) x 7.6 words/lines) = 489 Words
Figure 1: (51.0+10mm) x (2.2 words/mm) x 1 column + 14 words in caption = 148 Words
Figure 2: (47.9+10mm) x (2.2 words/mm) x 1 column + 19 words in caption = 146 Words
Figure 3: (61.0+10mm) x (2.2 words/mm) x 2 columns + 26 words in caption = 338 Words
Figure 4: (60.7+10mm) x (2.2 words/mm) x 2 columns + 26 words in caption = 337 Words
Figure 5: (59.3+10mm) x (2.2 words/mm) x 2 columns + 26 words in caption = 331 Words
Figure 6: (61.6+10mm) x (2.2 words/mm) x 2 columns + 26 words in caption = 341 Words
Figure 7: (59.9+10mm) x (2.2 words/mm) x 2 columns + 26 words in caption = 334 Words
Figure 8: (66.3+10mm) x (2.2 words/mm) x 2 columns + 12 words in caption = 348 Words
Figure 9: (50.9+10mm) x (2.2 words/mm) x 1 column + 39 words in caption = 173 Words
Figure 10: (83.6+10mm) x (2.2 words/mm) x 2 columns + 31 words in caption = 443 Words

Abstract: 151 Words

Submitted for consideration at the 37th International Symposium on Combustion, Dublin, 2018

Abstract

High pressure oxidation of 3-pentanol is investigated in a jet-stirred reactor and in a shock tube. Experiments in the reactor were carried out at 10 atm, between 730–1180 K, for equivalence ratios of 0.35, 0.5, 1, 2, 4 and 1000 ppm fuel, at a constant residence time of 0.7s. Reactant, product and intermediate species mole fractions were recorded using Fourier transform infrared spectroscopy (FTIR) and gas chromatography (GC). Ignition delay times were measured for 3-pentanol/O_2 mixtures in argon in a shock tube at 20 and 40 bar, in a temperature range of 1000–1470 K and for equivalence ratios of 0.5, 1 and 2. The fuel did not show any low-temperature reactivity under these conditions in neither experimental set-up and produced various aldehydes and ketones as well as the olefin 2-pentene as intermediates. A kinetic sub-mechanism is developed in order to represent the present data and analyze the reaction pathways.

Keywords: 3-pentanol, kinetics, jet-stirred reactor, shock tube

1. Introduction

Alcohols constitute an important family of potential biofuels that can be synthesized from renewable resources. Recently larger alcohols have been the focus of many studies due to their higher energy density and better solubility in gasoline. Alcohols up to C_4 have been extensively studied so far, however fewer studies are available for larger ($C \geq 5$) alcohols. As far as amyl alcohols are concerned, 1-pentanol, iso-pentanol and 2-methyl-1-butanol have already been investigated experimentally in the literature in terms of speciation [1-4], laminar burning velocity [5-7] and ignition delay times [7-10]. These isomers have different oxidation tendencies depending on their structure. Secondary C_5 alcohols such as 3-pentanol are much less studied. Köhler et al. [11] investigated oxidation of a 1-, 2- and 3-pentanol doped hydrogen flat flame using molecular-beam mass spectrometry. Li et al. [12] measured laminar flame speeds of 1-, 2- and 3-pentanol. The aim of this study is to provide new kinetic data through a detailed product analysis of 3-pentanol in a jet-stirred reactor (JSR) and by measuring ignition delay times behind reflected shock waves, for the first time. A chemical kinetic mechanism is developed and used to represent the present data.

2. Experimental

2.1. Jet-stirred reactor (Orléans)

The jet-stirred reactor (JSR) used in this work has been described previously [13]. It consists in a fused silica jet-stirred reactor that can be heated up to 1250 K and pressurized at 10 atm, located inside a regulated electrical resistance oven of ≈ 3kW itself surrounded by insulating ceramic wool and a stainless-steel pressure-resistant jacket. The liquid fuel is brought by an HPLC pump to the entrance of a home-made vaporization system where it is atomized by a nitrogen flow (50L/h) and then vaporized in a heated chamber ($T_{vaporiser}$ = 120°C). The fuel+N_2 mixture is carried to the reactor

by a quartz capillary. The oxidizing stream (oxygen + nitrogen) is conveyed independently to prevent any reactions prior to the reactor. All gaseous flowrates are regulated by thermal mass flow controllers (Brooks 5850E). The two flows merged right ahead of the reactor, in which they are injected by four nozzles that ensure stirring. The sampling system, which consists of a fused-silica protected S-type thermocouple and a low pressure sonic fused silica probe, can be moved along a vertical axis to check the temperature and the composition homogeneity inside the reactor. Residence time distribution studies have shown that under the conditions of the present study the reactor is operating under macro-mixing conditions [13]. Samples are analyzed online by means of FTIR and stored at low pressure for offline GC analysis. The fuel (CAS number 584-02-1, 98% purity) was supplied by Sigma Aldrich and high purity gases (oxygen and nitrogen from Air Liquide, oxygen 99.995% pure and nitrogen with <1000 ppm Ar, <100 ppm H_2O, <50 ppm O_2, <5 ppm H_2) were used for this study. The carbon balance was checked after each experiment and was found to be within ±10%. Uncertainties on the species mole fractions is due to several factors described in [14], such as reactor temperature (< 10 K), pressure (±0.1 atm), residence time (< 5%), etc., and are very difficult to evaluate precisely, these are estimated to be around ±15%. Intermediate species observed include, 3-pentanone, formaldehyde, acetaldehyde, propanal, ethylene, methane, 2 pentene (cis and trans isomers). Butanone, methylvinylketone, butadiene, methacrolein and ethylvinylketone are quantified as well but to a lesser extent, and some in trace amounts. All experiments were performed at 10 atm operating pressure and between 700 and 1180 K. Also, few experiments were performed down to 500 K for the lean mixture and no low temperature reactivity was observed.

2.2. High pressure shock tube (Nevers)

The ignition delay times were measured in a high-pressure shock tube in DRIVE over a temperature range of 1030–1460 K at 20 bar and 40 bar. Mixtures of 3-pentanol (1%) + O_2 diluted in

argon are tested for equivalence ratios of 0.5, 1 and 2. The tube consists of a stainless-steel tube with an inner diameter of 50 mm and separated into two parts, the driver section (length: 4m) and the driven section (length: 5m) by a double stainless-steel diaphragm [15]. The tested mixtures are prepared into two stainless-steel tanks based on the partial pressure method using high purity gases (greater than 99.995% for Ar, O_2 and He) and 3-pentanol with a purity of 98%. To prevent any contamination, the facility includes a vacuum system, a roughing pump and a turbo-molecular pump, which pumps down the tube, the manifold, the stainless-tanks, the manifold and the previously frozen fuel tank below 5 Pa. In order to avoid any condensation of the fuel, the tube, the tanks and the manifold are heated up to 80 °C to allow the partial pressure of the 3-pentanol be at least three times lower than its vapor pressure. The data acquisition system has a frequency of 1 MHz and includes a NI Compact RIO which records the pressure signals from four individual piezoelectric pressure transducers PCB 113B22 in order to calculate the shock velocity and from a Kistler piezoelectric pressure transducer (603B1) located at the end-wall to calculate the ignition delay time and determine post-shock pressure, P_5. It is defined as the time interval between the rebound of the shock wave at the end-wall and the onset of combustion, commonly defined by a sudden change in pressure (inflection point), see Figure 1. Post-shock temperature, T_5, is calculated from the shock wave velocity and the initial conditions based on the 1-D shock relations and the species thermodynamics using the chemical equilibrium software Gaseq [16] with an accuracy of ±1% which corresponds to ±10–15K according to the uncertainty calculation proposed by Petersen et al. [17].

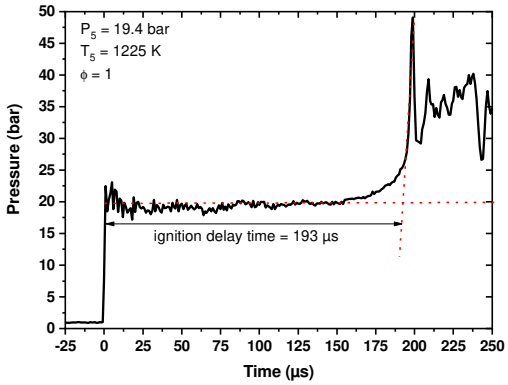

Figure 1. Ignition delay time measurement, initial mixture: 1% fuel, 7.5% O_2, balance argon

3. Kinetic modeling

The kinetic model used in the simulations is constructed by introducing a sub-mechanism of 3-pentanol into an in-house C_0-C_4 base (258 species in 1695 reactions). This base is already involved in our recent studies, e.g. [18, 19]. The thermochemical parameters of the fuel and related species were evaluated using Thergas [20], which uses the group additivity methods proposed by Benson [21]. All kinetic simulations were performed using Chemkin-II [22] using PSR and SENKIN modules (constant V) for the JSR and shock tube simulations, respectively. Fuel reactions include water elimination, H_2 elimination, unimolecular dissociations into radicals, and bimolecular initiation reactions with O_2, and hydrogen abstraction reactions by radicals. Through these latter reactions, the fuel can yield four distinct radicals three of which are considered in this study. These are named pent3oh-1 (where the radical site is in γ position with respect to the carbon bearing the –OH group), pent3oh-2 (radical site in β position) and pent3oh-3, which is the α-hydroxyalkyl radical. The 3-pentoxy radical is not included given that its formation would not be favorable because of the large bond dissociation energy associated to this C–H bond (~105 kcal/mol). For the H-abstraction reactions by important radicals such as OH, H, CH_3 and HO_2 yielding the pent3oh-3 radical, rate constants were taken in analogy with sec-butanol from literature [23-25]. As far as the γ and β radicals are concerned, rate constants are

estimated as for primary and secondary C–H, respectively as in alkanes. Both the mechanism and thermochemistry files are provided as supplementary material, with corresponding references therein. Unimolecular fuel reactions are not of importance in the present JSR conditions and have a negligible contribution at high temperature ignition delays. One of the main oxygenated intermediate species observed in 3-pentanol oxidation is 3-pentanone, which is a product of the β-scission of the α-hydroxyalkyl radical. Therefore a sub-mechanism involving reactions of 3-pentanone and ethyl vinyl ketone were also considered, partly in analogy with our previous study on butanone oxidation [26], which itself is also observed as an intermediate species.

4. Results and discussion

JSR experiments

Figure 2 represents fuel mole fraction at different equivalence ratios investigated. Reactivity starts being observed around 760 K for all mixtures. While almost all fuel is consumed by 880 K for the lean mixtures, conversion for the φ = 4 mixture, at this temperature is around 70%. It is to be noted that some additional experiments were performed between 500–700 K for the φ = 0.5 mixture, and no low-temperature reactivity was observed.

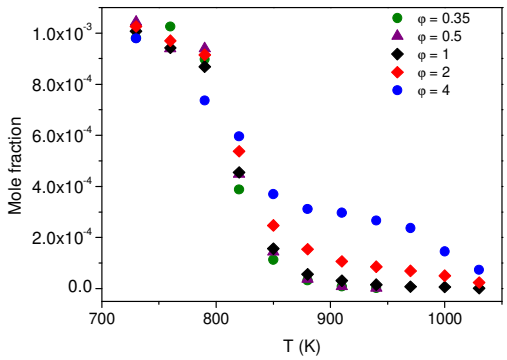

Figure 2. Fuel mole fraction at all equivalence ratios investigated (P = 10 atm, and τ = 0.7 s).

Figures 3–7 represent mole fractions of the major species quantified for mixtures φ = 0.35, 0.5, 1, 2 and 4. The major hydrocarbon products quantified are C_2H_4, CH_4 and 2-C_5H_{10}. For the latter cis- and trans- isomers were quantified and simulated but plotted as a sum of both. The major oxygenated intermediates include formaldehyde, acetaldehyde, propanal and 3-pentanone. The latter ketone is a direct product of the fuel chemistry as it is produced from the β-scission of the (tertiary) fuel radical namely pent3oh-3. Its mole fraction is well predicted by the model although a discrepancy of about 25% is observed for the peak value at φ = 0.35 and 0.5. The same radical also leads to the formation of another ketone intermediate, 2-butanone (assuming a fast isomerization of but-1-en-2-ol during sampling), which is quantified within 15–70 ppm in our experiments. Unsaturated ketones ethyl vinyl ketone (pent-1-en-3-one) and methyl vinyl ketone are observed in much smaller quantities, less than 10 ppm. Another major intermediate directly related to fuel radical decomposition is 2-pentene, quantified around 70 ppm at φ = 4.

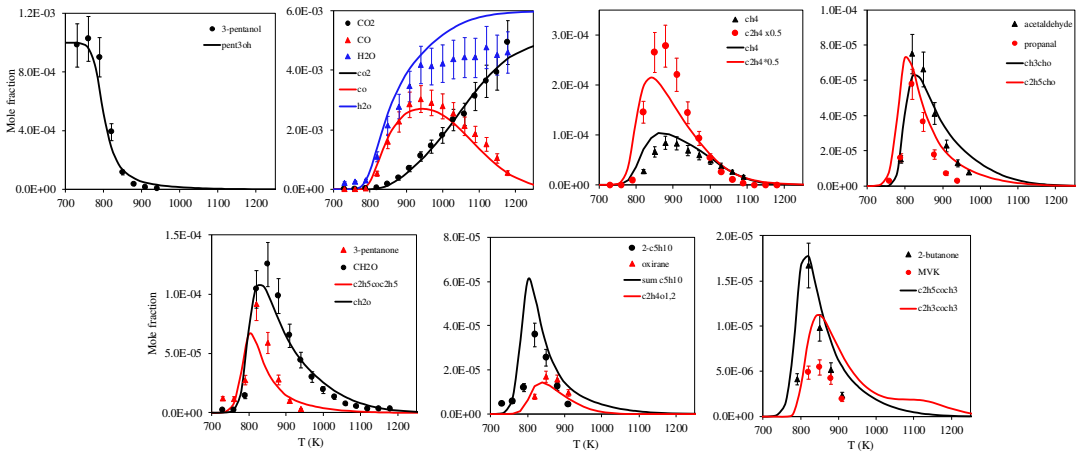

Figure 3. Species mole fractions as a function of temperature (K) for the φ = 0.35 mixture (*P* = 10 atm, and τ = 0.7 s).

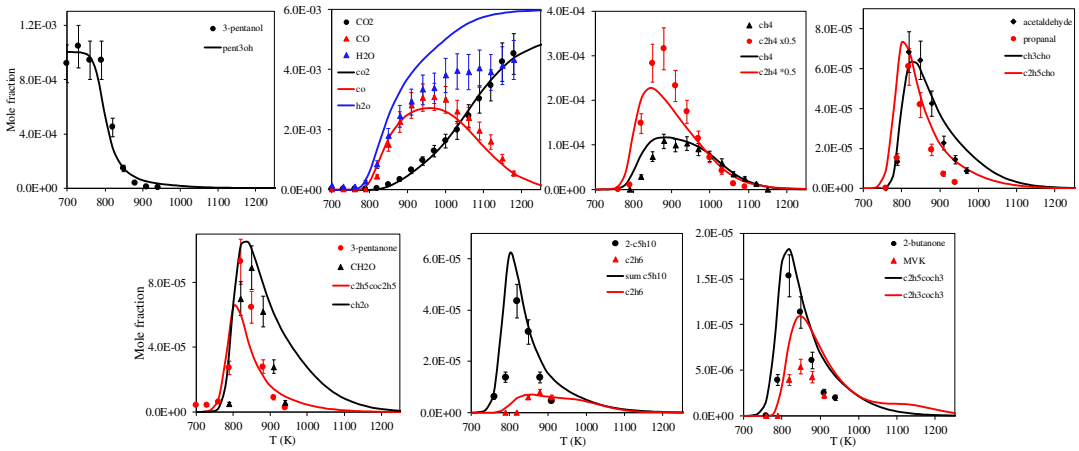

Figure 4. Species mole fractions as a function of temperature (K) for the φ = 0.5 mixture (*P* = 10 atm, and τ = 0.7 s).

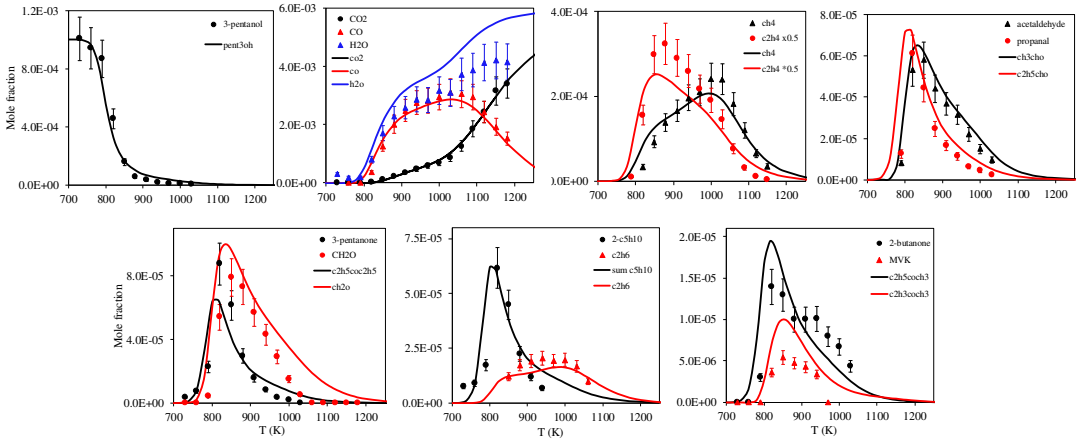

Figure 5. Species mole fractions as a function of temperature (K) for the φ = 1 mixture (*P* = 10 atm, and τ = 0.7 s).

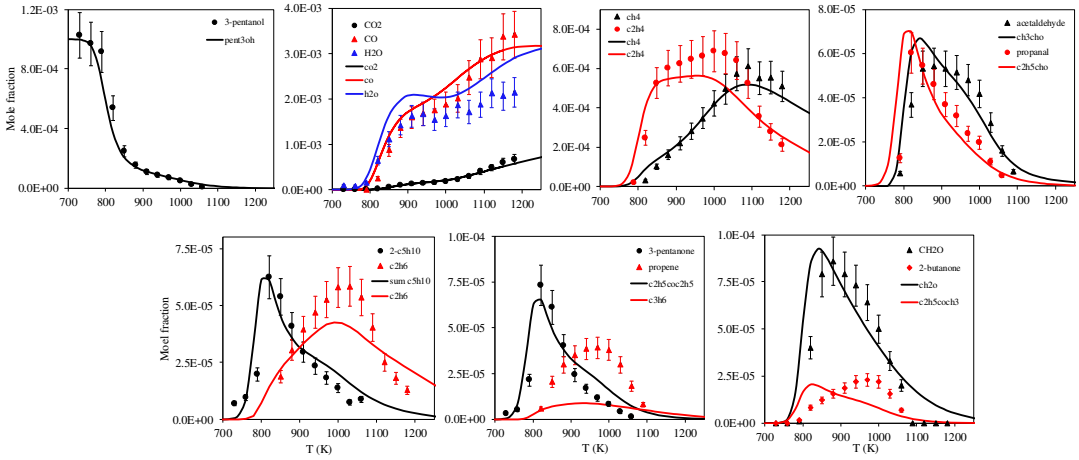

Figure 6. Species mole fractions as a function of temperature (K) for the φ = 2 mixture (P = 10 atm, and τ = 0.7 s).

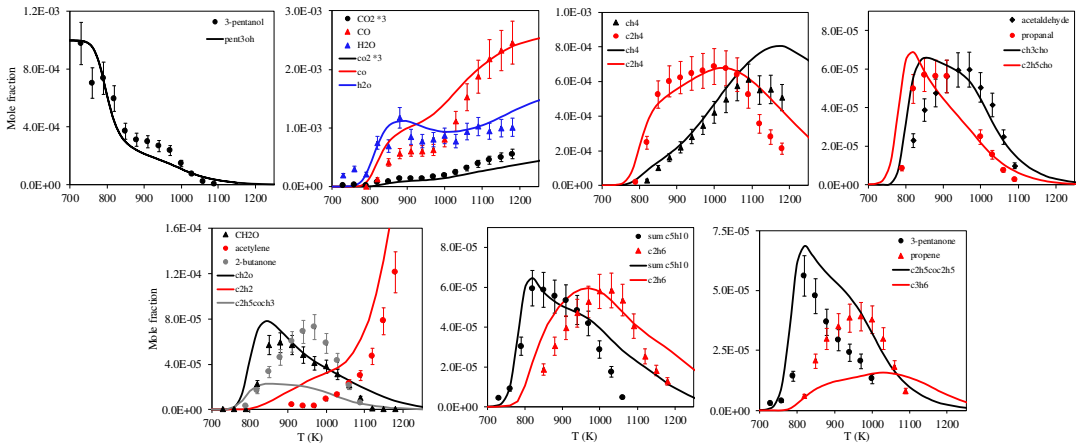

Figure 7. Species mole fractions as a function of temperature (K) for the φ = 4 mixture (P = 10 atm, and τ = 0.7 s).

Figure 8 shows the primary decomposition pathways of 3-pentanol for the stoichiometric mixture at 800 K. A similar figure can be found in supplementary material covering the analysis to φ = 0.35 and φ = 4 mixtures. Fuel is mainly consumed by the attack of OH radicals (75% of the flux), and H, HO_2 as well CH_3 radicals to a lesser extent. Although the bond energy for a tertiary C–H bond neighboring the –OH group is weaker than primary and secondary C–H sites available, given the

presence of 4 equivalent secondary C–H sites, the pent3oh-2 radical formation is more favored and corresponds to 53% of the flux. This pent3oh-2 radical forms 2-pentene or propanal by β-scission of C–O and C–C bonds, respectively. All 2-pentene observed is formed this way. On the other hand, the pent3oh-1 radical forms mostly ethylene and C_2H_5CHOH radical via β-scission This radical, in turn, can give vinyl alcohol and propanal by C–C and O–H bond breaks, respectively. However, propanal formation is largely due to the pathway from pent3oh-2 radical, which is more abundant. The ketones (butanone and 3-pentanone) observed in this study are both products of the chemistry following the formation of pent3oh-3 radical, as shown. Butanone is minor compared to 3-pentanone (20% of the flux of pent3oh-3 radical) except at φ = 4 where both species are comparable. Methyl vinyl ketone (MVK) was quantified in trace amounts, around 5–6 ppm which can be seen in figures 2–4. On the other hand, 3-pentanone amounts up to around 90 ppm for the lean mixtures, and pent-1-en-3-one is observed in trace amounts.

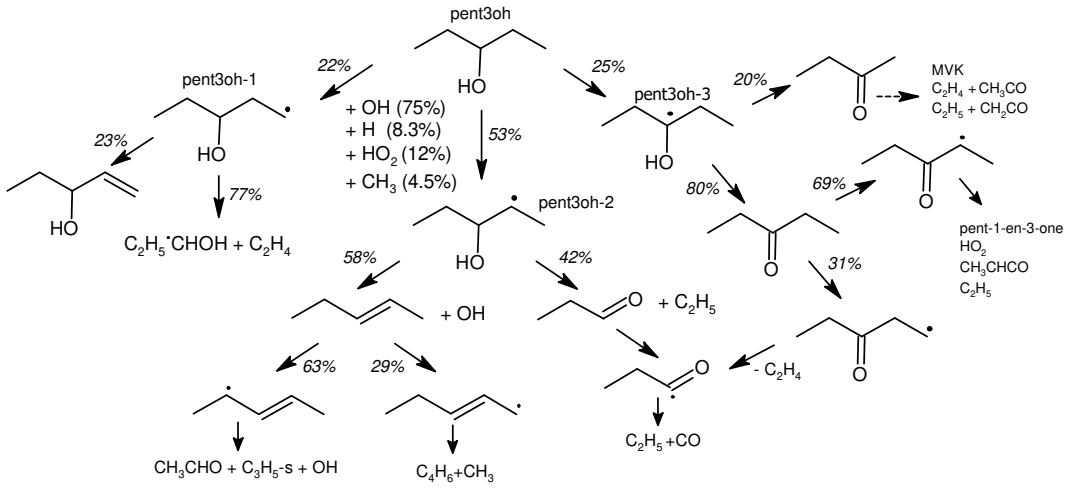

Figure 8. Main fuel decomposition pathways at 70% fuel conversion, φ = 1

Kinetic model predictions are generally in good agreement with experimental results. However, some discrepancies are observed, for example with propene which is under-predicted by a factor of 3, probably because of a missing pathway. Also, for the φ = 4 mixture, there is an over-prediction of

reactivity in the fuel mole fraction profile between a small temperature window of 880–1000 K. This results in an over-prediction of the CO profile within the same temperature range. Given the shape of water profile correctly predicted, this small discrepancy is probably not a result of H-abstraction reactions by OH consuming the fuel and other abundant intermediates such as propanal, formaldehyde, etc. but rather an under-estimation of a species likely accumulating and decreasing the overall reactivity. Also, experimental profiles of butanone and 3-pentanone do not quite show the same tendency at $\varphi = 2$ and 4 as opposed to lean and stoichiometric mixtures and the model prediction for butanone in these rich cases is shifted towards lower temperatures. This observation might suggest an unexplored formation path for this ketone rather than a problem with the branching ratio with the decomposition of the pent3oh-3 radical or the consumption pathways. Water profiles are over-predicted by about 20% for the lean and stoichiometric mixtures, probably because of the higher uncertainty in H_2O mole fractions measured at high quantities.

A comparison between different isomers of pentanol investigated in our JSR is presented in figure 9, in terms of fuel mole fraction profiles. According to this, on a logarithmic scale, one can easily note the difference in reactivity between 1-pentanol (pent1oh) and iso-pentanol (butoh3m). The reactivity of 3-pentanol lies between these. A major oxygenated intermediate in 1-pentanol oxidation is pentanal [1], and both produce reactive alkyl radicals during oxidation, on the other hand iso-pentanol, due to its structure, produces less reactive intermediates, such as iso-butene [2]. An interesting feature in 3-pentanol oxidation, which is a secondary alcohol, is that it produces ketone species as well as aldehydes, unlike primary alcohols where the structure does not allow the formation of a ketone with the same carbon number.

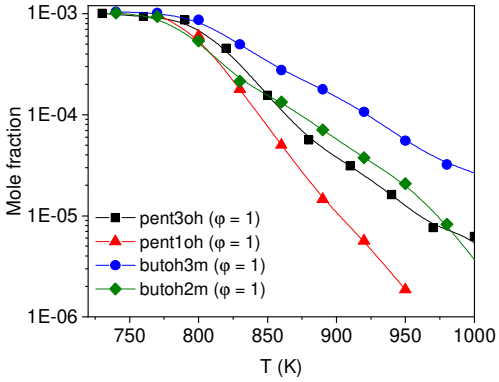

Figure 9. Experimental fuel mole fraction profiles of 3-pentanol, 1-pentanol [1], 3-methyl-1-butanol [2] and 2-methyl-1-butanol [3] at 10 atm, 1000 ppm of initial mole fraction and $\tau = 0.7$s for all experiments:, lines are added to guide the eye.

Shock tube experiments

Mixtures of 1% 3-pentanol in O_2/Ar are tested in a high-pressure shock tube at 20 and 40 bar of pressure and equivalence ratios of 0.5, 1 and 2 between 1000 and 1460 K. No pressure rise was recorded after the reflected shock wave prior to the main ignition event. Kinetic model and experiment comparisons are presented in figure 10. The influence of the experimental conditions (temperature, pressure and equivalence ratio) on ignition delay times is observed to be as expected: the ignition delay times decrease with increasing pressure and temperature as well as increasing oxygen concentration. The effect of equivalence ratio is more apparent at 20 bar than at 40 bar, experimentally. Kinetic model agrees very well with the data for the mixtures $\varphi = 0.5$ and 1, however predicts longer ignition delay times regardless of the pressure as far as the $\varphi = 2$ mixtures are concerned, although the global activation energy is correct. For example at 1250 K, this over-prediction at $\varphi = 2$ is less than a factor of 2 at 20 bar and a factor of 2 at 40 bar. We can also note that at the lowest temperatures investigated ($\approx$ 1050–1100 K) experimental ignition delays tend to converge while the model predicts a more pronounced dependence on equivalence ratio over all temperature range.

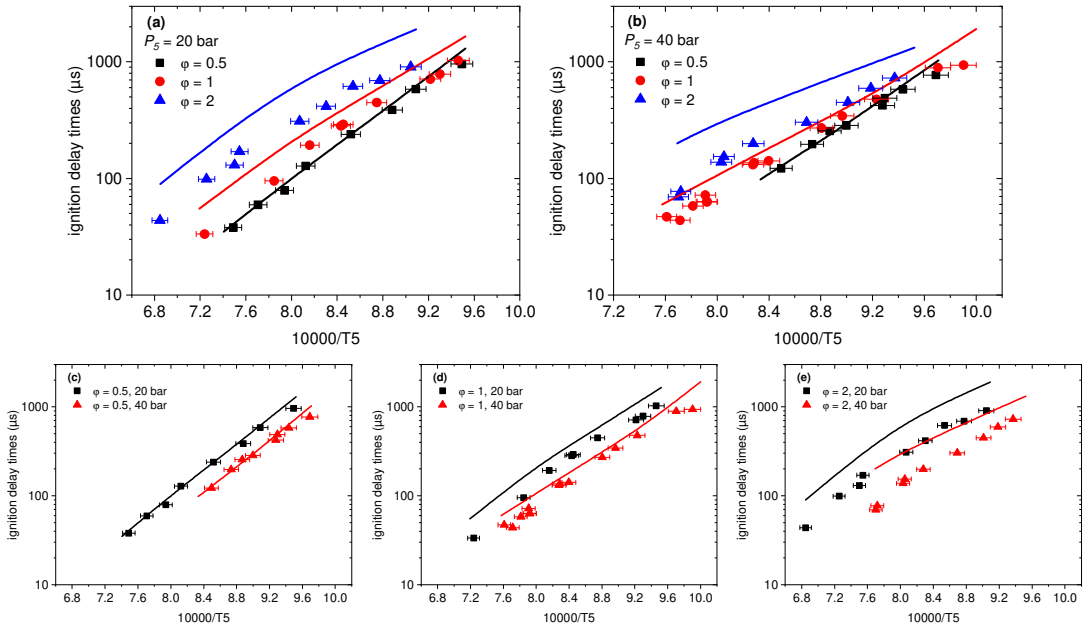

Figure 10. Ignition delay times of 1% 3-pentanol/O_2/Ar mixtures at (a) 20 bar and (b) 40 bar. Lower panel (c–e) shows the effect of pressure for a given equivalence ratio.

Sensitivity analysis at 1200 K; φ = 1 and 40 bar (Figure S3) shows that among the fuel-related reactions, H-abstraction by OH and H producing the primary radical inhibit reactivity while H-abstraction by HO_2 producing pent3oh-2 (secondary) radical promote reactivity. Beta decomposition of the latter gives ethyl radicals and propanal, which itself yields ethyl radicals, promoting reactivity by supplying H atoms to the system. Part of the pent3oh-2 yields the stable molecule 2-pentene and OH radicals, inhibiting overall reactivity. Branching between these pathways could be one factor affecting the delays, which is based on estimations in this study. Pathways of fuel and fuel radical decomposition under these conditions can also be found in Figure S4.

5. Conclusion

High pressure oxidation of 3-pentanol is investigated experimentally in a JSR and in a shock tube, for the first time. Mole fraction profiles of the reactants, final products, and stable intermediates are identified and measured by gas chromatography, mass spectrometry, and Fourier transform

infrared spectrometry after sonic probe sampling at five equivalence ratios. Ignition delay times are measured for 1% fuel in O_2/Ar mixtures at 20 and 40 bar for 3 equivalence ratios. Under the investigated conditions, 3-pentanol did not show any cool flame behavior and is found to produce various aldehydes and ketones as well as the olefin 2-pentene as one of its C_5 intermediates. A sub-mechanism for 3-pentanol was developed in order to represent the data with globally good performance, however some discrepancies were observed in species profiles, which suggest further work. Experimental fuel profile is compared with previous oxidation studies of 1-pentanol, iso-pentanol and 2-methylbutanol under same conditions and the global reactivity of 3-pentanol is found to be between that of 1-pentanol and iso-pentanol. Moreover, laminar burning velocities of 3-pentanol measured by Li et al. [12] were also simulated with the present model (Figure S1) with reasonably good agreement. More data would certainly be useful, such as detailed speciation at lower pressure, pyrolysis, or ignition delay data at lower temperatures of interest in order to unravel more about 3-pentanol kinetics and further refine the kinetic mechanism.

6. Acknowledgements

Authors gratefully acknowledge funding received from Bourgogne council under the PARI2 program (No 2016-9201AAO048S01891) and Labex Caprysses (convention ANR-11-LABX-0006-01)

7. Supplementary material

The kinetic mechanism and thermodynamic data in Chemkin format

List of figures

References

[1] C. Togbé, F. Halter, F. Foucher, C. Mounaim-Rousselle, P. Dagaut, Proceedings of the Combustion Institute, 33 (2011) 367-374.

[2] G. Dayma, C. Togbé, P. Dagaut, Energy & Fuels, 25 (2011) 4986-4998.

[3] Z. Serinyel, C. Togbé, G. Dayma, P. Dagaut, Combustion and Flame, 161 (2014) 3003-3013.

[4] G. Wang, W. Yuan, Y. Li, L. Zhao, F. Qi, Combustion and Flame, 162 (2015) 3277-3287.

[5] Q. Li, C. Tang, Y. Cheng, L. Guan, Z. Huang, Energy & Fuels, 29 (2015) 5334-5348.

[6] D. Nativel, M. Pelucchi, A. Frassoldati, A. Comandini, A. Cuoci, E. Ranzi, N. Chaumeix, T. Faravelli, Combustion and Flame, 166 (2016) 1-18.

[7] S. Park, O. Mannaa, F. Khaled, R. Bougacha, M.S. Mansour, A. Farooq, S.H. Chung, S.M. Sarathy, Combustion and Flame, 162 (2015) 2166–2176.

[8] K.A. Heufer, J. Bugler, H.J. Curran, Proceedings of the Combustion Institute, 34 (2013) 511-518.

[9] S. Mani Sarathy, S. Park, B.W. Weber, W. Wang, P.S. Veloo, A.C. Davis, C. Togbe, C.K. Westbrook, O. Park, G. Dayma, Z. Luo, M.A. Oehlschlaeger, F.N. Egolfopoulos, T. Lu, W.J. Pitz, C.-J. Sung, P. Dagaut, Combustion and Flame, 160 (2013) 2712-2728.

[10] C. Tang, L. Wei, X. Man, J. Zhang, Z. Huang, C.K. Law, Combustion and Flame, 160 (2013) 520-529.

[11] M. Köhler, T. Kathrotia, P. Oßwald, M.L. Fischer-Tammer, K. Moshammer, U. Riedel, Combustion and Flame, 162 (2015) 3197-3209.

[12] Q. Li, E. Hu, X. Zhang, Y. Cheng, Z. Huang, Energy & Fuels, 27 (2013) 1141-1150.

[13] P. Dagaut, M. Cathonnet, J.P. Rouan, R. Foulatier, A. Quilgars, J.C. Boettner, F. Gaillard, H. James, Journal of Physics E: Scientific Instruments, 19 (1986) 207.

[14] Z. Serinyel, C. Togbé, A. Zaras, G. Dayma, P. Dagaut, Proceedings of the Combustion Institute, 35 (2015) 507-514.

[15] H. El Merhubi, A. Kéromnès, G. Catalano, B. Lefort, L. Le Moyne, Fuel, 177 (2016) 164-172.

[16] C. Morley, in, 2005.

[17] E.L. Petersen, M. Rickard, J. A. , M. Crofton, W. , E. Abbey, D. , M. Traum, J. , D. Kalitan, M. , Measurement Science and Technology, 16 (2005) 1716.

[18] Z. Serinyel, C. Togbé, G. Dayma, P. Dagaut, Energy & Fuels, 31 (2017) 3206-3218.

[19] S. Thion, C. Togbé, Z. Serinyel, G. Dayma, P. Dagaut, Combustion and Flame, 185 (2017) 4-15.

[20] C. Muller, V. Michel, G. Scacchi, G.M. Côme, Journal de chimie physique et de physico-chimie biologique, 92 (1995) 1154-1178.

[21] S.W. Benson, Thermochemical Kinetics, Wiley, New York, 1976.
[22] R.J. Kee, F.M. Rupley, J.A. Miller, in: SAND89-8009, Sandia National Laboratories, Livermore (CA), 1989.
[23] K. Yasunaga, T. Mikajiri, S.M. Sarathy, T. Koike, F. Gillespie, T. Nagy, J.M. Simmie, H.J. Curran, Combustion and Flame, 159 (2012) 2009-2027.
[24] S.M. Sarathy, S. Vranckx, K. Yasunaga, M. Mehl, P. Oßwald, W.K. Metcalfe, C.K. Westbrook, W.J. Pitz, K. Kohse-Höinghaus, R.X. Fernandes, H.J. Curran, Combustion and Flame, 159 (2012) 2028-2055.
[25] H.-H. Carstensen, A.M. Dean, Development of Detailed Kinetic Models for the Thermal Conversion of Biomass via First Principle Methods and Rate Estimation Rules, in: Computational Modeling in Lignocellulosic Biofuel Production, American Chemical Society, 2010, pp. 201-243.
[26] S. Thion, P. Diévart, P. Van Cauwenberghe, G. Dayma, Z. Serinyel, P. Dagaut, Proceedings of the Combustion Institute, 36 (2017) 459-467.